Arabinoxylan Microspheres: Structural and Textural Characteristics

Ana L. Martínez-López, Elizabeth Carvajal-Millan, Mario Miki-Yoshida, Lorena Alvarez-Contreras, Agustín Rascón-Chu, Jaime Lizardi-Mendoza and Yolanda López-Franco.

Abstract

The aim of this research was to study the structural and textural characteristics of maize bran arabinoxylan (MBAX) microspheres. The laccase-induced cross-linking process was monitored by storage (G') and loss (G'') moduli changes in a 4% (w/v) MBAX solution. The G' and G'' values at the plateau region were 215 and 4 Pa, respectively. After gelation, the content of ferulic acid dimers decreased from 0.135 to 0.03 µg/mg MBAX, suggesting the formation of ferulated structures unreleased by mild alkaline hydrolysis. MBAX microspheres presented an average diameter of 531 µm and a swelling ratio value (q) of 18 g water/g MBAX. The structural parameters of MBAX microspheres were calculated from equilibrium swelling experiments, presenting an average mesh size of 52 nm. Microstructure and textural properties of dried MBAX microspheres were studied by scanning electron microscopy and nitrogen adsorption/desorption isotherms, respectively, showing a heterogeneous mesoporous and macroporous structure throughout the network.

Keywords: maize bran arabinoxylans; microspheres; ferulic acid; microstructure.

Introduction

Microencapsulation of bioactive agents has recently become a relevant alternative to develop novel oral delivery systems. Microspheres can encapsulate many types of drugs, including small molecules, proteins and nucleic acids, thus providing

improved oral bioavailability [1]. While a variety of devices have been used as a carrier material for bioactive agents, biopolymer-based microspheres offer several advantages. Due to their attractive biodegradable, biocompatible, non-toxic and hydrophilic properties and their mild cross-linking conditions, natural polysaccharides such as chitosan, alginate, dextran, among others, have received increasing attention as oral delivery systems [2–7]. Hydrogel polysaccharides, particularly in the form of microspheres, have been extremely useful in the controlled release of bioactive agents and their targeting to selective sites [8,9].

Hydrogels are three-dimensional polymer networks capable of imbibing large amounts of water [9]. Covalently cross-linked gels generally present high water absorption capacity, absence of pH or electrolyte susceptibility and exhibit no syneresis after long periods of storage [10]. An example of covalently cross-linked gels is the product of oxidative coupling of ferulated arabinoxylan chains. Arabinoxylans (AX) are important cereal non-starch polysaccharides constituted of a linear backbone of β-(1→4)-linked D-xylopyranosyl units to which α-L arabinofuranosyl substituents are attached through O-2 and/or O-3 [10]. Some of the arabinose residues are ester-linked on (O)-5 to ferulic acid (FA, 3-methoxy-4 hydroxycinnamic acid) [11]. One of the most important properties of AX is the ability to form gels by covalent cross-linking involving FA oxidation by either chemical (ferric chloride, ammonium persulphate) or enzymatic (peroxidase/H_2O_2, laccase/O_2) free radical-generating agents [10,12–15]. This oxidation allows the coupling of AX chains through the formation of dimers and trimers of FA (di-FA, tri-FA), generating an aqueous three-dimensional network (Figure 1). The content of covalent bonds in the gel is determined by the extent of oxidative coupling of FA and

can be quantified by the formation of di-FA and tri-FA [16]. Five isomeric forms of di-FA structures have been reported in AX gels: 5-5'-, 8-5'-benzo-, 8-O-4'-, 8-5'- and 8-8'- [17,18] and only one tri-FA: 4-O-8', 5-5'- [19]. In addition to covalent bonds (di-FA and tri-FA), physical interactions between AX chains can contribute to the gelation process [12,16].

Previous studies have demonstrated that AX gels formed via the oxidative cross-linking using laccase could be employed for controlled release of model proteins [17,19,20], methyl xanthine [21] and lycopene [22], making AX hydrogels good candidates for the design of novel colon-specific delivery systems. Recently, the formation of laccase-induced AX microspheres stabilized by covalent linkages has been reported for the first time [23]. AX microspheres present several advantages compared with other polysaccharide microspheres as covalently cross-linked networks are strong, form quickly, are stable upon heating and exhibit no syneresis after extended storage [10]. However, the structural and textural characteristics of AX microspheres have not been reported yet. In this study, maize bran arabinoxylans (MBAX) presenting gelling capability were used to prepare MBAX microspheres which were then investigated in terms of their structural and textural characteristics.

Figure 1. Schematic representation of the covalent cross-linking of ferulated arabinoxylans. Ferulated arabinoxylans (a) in solution and (b) in gel. Covalent cross-linking through a 5,5 diferuloyl moiety in the gel is presented as an example. α-L-Araf = α-L-arabinofuranose, β-D-Xylp = β-D-xylopyranose.
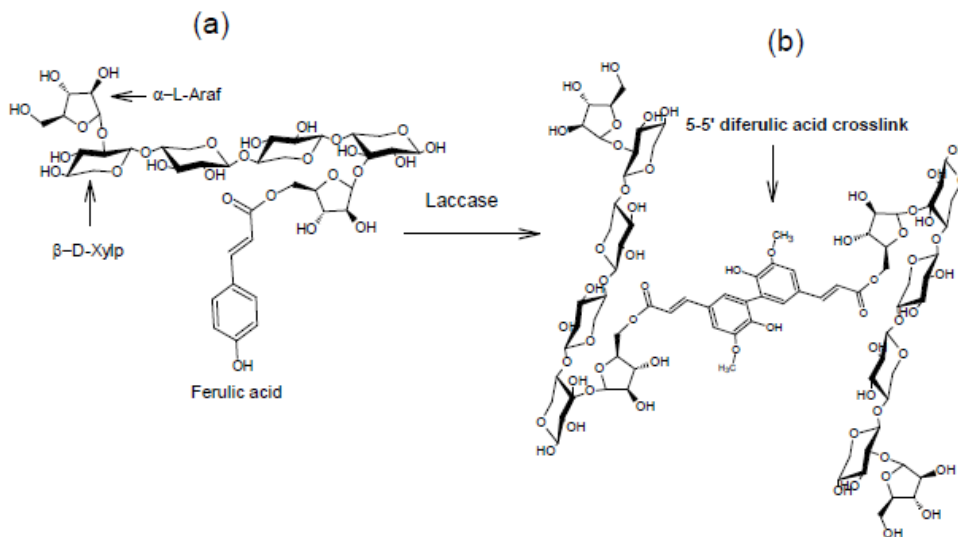
**Results and Discussion**

MBAX Cross-Linking:

The MBAX gelation was monitored by storage (G') and loss (G") moduli changes in a 4% (w/v) polysaccharide solution undergoing oxidative gelation by laccase (Figure 2a). The gelation profile vs. time exhibited an initial increase of G' modulus, followed by a plateau region. The rheological measurements indicated that the gelation time (tg), calculated from the crossover of the G' and G" curves (G' > G") was 4 min. The tg value indicates the sol/gel transition point and at this point G' = G" or tan δ = G"/G' = 1 [24]. The values of G' and G" at the plateau region were 215 and 4 Pa, respectively. The tan δ value decreased during MBAX gelation (Figure 2a) indicating the presence of an elastic covalent system. The mechanical spectra of the MBAX gel obtained for 6 h gelation (Figure 2b), was typical of a solid-like material with a linear G' independent of frequency and G" much smaller than G" and dependent of frequency. This frequency-independent behavior is indicative of a stable, cross-linked network and similar to that

reported for AX gels [14,25]. The high G' value of MBAX gel has been attributed to the covalent cross-linking content and to the physical entanglement of MBAX chains [17]. The extent of covalent cross-linking in MBAX gels was determined by the content of ferulate monomer and total di-FA and tri-FA before and after 6 h of gelation (Table 1). FA was oxidized (82% of initial FA content) during the gelation process. After gelation, the di-FA content in MBAX gels did not increase, but rather decreased from 0.135 to 0.03 µg/mg MBAX. The tri-FA was present only in trace quantities (0.003 µg/mg MBAX). Nevertheless, the tan δ (G"/G') values confirm the formation of a true gel after laccase treatment (Figure 2b). This behavior in MBAX gels has been previously reported by several authors [14,15,24–26]. These authors attributed this result to the formation of ferulated cross-linking structures which cannot be released by mild alkaline hydrolysis and/or to the participation of lignin residues in the formation of MBAX gel. The relative percentages of each di-FA structures in MBAX gels were: 78%, 14% and 8% for the 8-5' (mainly in the benzofuran form), 5-5' and 8-O-4' structure, respectively. Previous research on MBAX gels induced by peroxidase/H_2O_2 system also reported the 8-5' di-FA structure as predominant [14].

Figure 2. (a) Monitoring the tan δ (X), storage (G'●) and loss (G"○) modulus of MBAX solution during gelation by laccase at 25 °C, 0.25 Hz and 5% strain; (b) Mechanical spectrum of MBAX gels at 6 h (G'●, G"○). Data obtained at 25 °C and 5% strain.
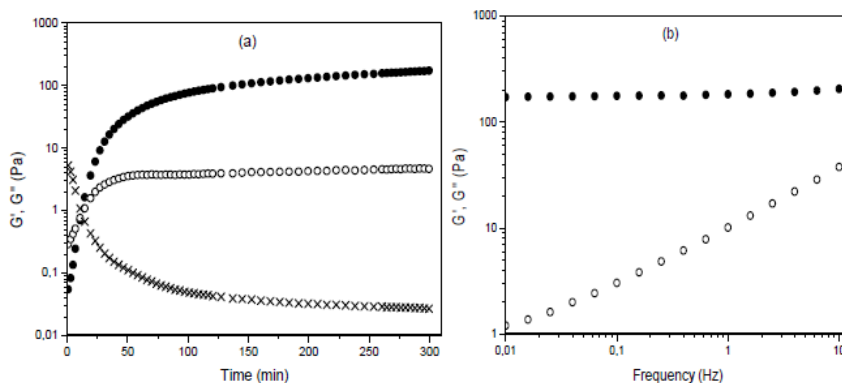
MBAS Microspheres:

The MBAX microspheres presented a size distribution from 350 µm up to 798 µm, with an average diameter of 531 µm (Figure 3a). These particle size values were similar to those reported for other polysaccharide microspheres such as alginate (350 µm) [27]. Optical micrographs of MBAX microspheres show a spherical shape and no aggregation of particles (Figure 3b). Secondary electron SEM images of cross-sectional MBAX microspheres is shown in Figure 3c,d. The microsphere morphology presented a three-dimensional and heterogeneous network structure, with irregular pores size and geometries (Figure 3c). The SEM micrograph of Figure 3d (magnification), shows clusters of interconnected nodular structures. The aggregation of nodular structures in clusters allows pore sizes of 10–70 nm, while the binding with other clusters leads to pores sizes on the macroporous order. It has been reported that for gels cross-linked via phenolic groups, the pore size is determined by the presence of nodular clusters [28–33]. Thus, the heterogeneous microstructure of MBAX microspheres could be attributed to the content and distribution of ferulic acid covalent cross-linking structures forming the MBAX network.

The swelling behavior of MBAX microspheres was followed for 30 min at 25 °C, with the equilibrium being reached between 8–12 min. This water dissolution mechanism of the MBAX microspheres was fitted to the Fick model. The n value was 0.19, indicating that the dissolution is due to a Fickian diffusion, where water penetration rate in the microsphere is lower than the polymer chain relaxation rate. The swelling ratio value (q) in MBAX microspheres was 18 g water/g MBAX, which is similar to the value reported for MBAX hydrogels (20 g water/g AX) [24]. Nevertheless, MBAX

microspheres showed a very short swelling time to reach equilibrium (12 min) compared to that reported for cylindrical MBAX hydrogels (15 h) [24]. This behavior could be explained in terms of an increase in the surface area-to-volume ratio in MBAX microspheres.

Figure 3. Characterization of MBAX microspheres. (a) Diameter distribution; (b) Optical microscope observation; (c and d) SEM images.
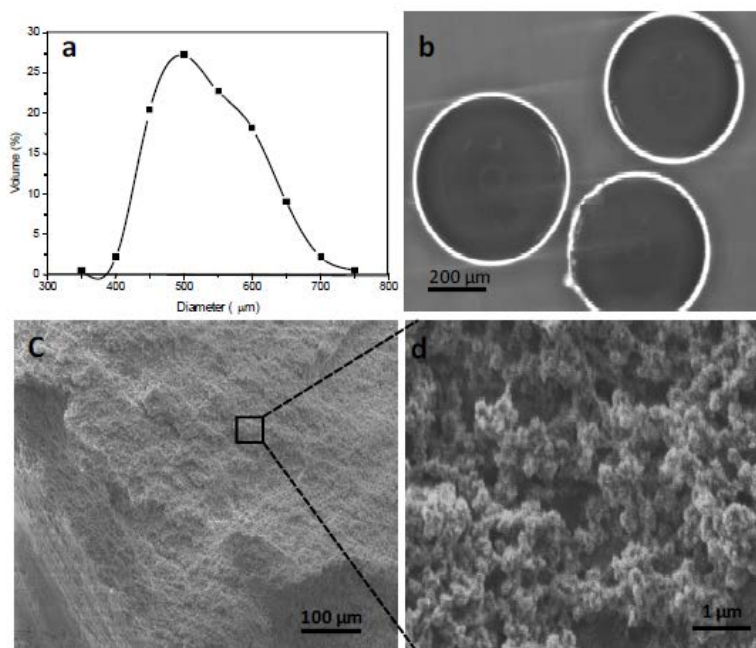
The molecular weight between two cross-links (Mc), the cross-linking density (pc) and the mesh size (ϑ) values of gelled MBAX are presented in Table 1. Similar structural parameters have been reported for maize bran and wheat bran arabinoxylan gels [14,34]. Higher mesh sizes values (201–331 nm) have been reported in laccase-induced wheat flour AX gels at lower polysaccharide concentrations (0.5%– 2% w/v) [17] and higher di-FA and tri-FA contents. The latter could be related to the high molecular weight reported for arabinoxylans from wheat flour (438 kDa) [17] in

comparison to the alkali-extracted arabinoxylans from maize bran (197 kDa) used in the present study [35].

Table 1. Characteristics of MBAX before and after 6 h of cross-linking process.

Characteristic	t = 0 h	t = 6 h
FA (μg/mg MBAX)	0.255 ± 0.017	0.045 ± 0.002
di-FA (μg/mg MBAX)	0.135 ± 0.011	0.03 ± 0.001
tri-FA (μg/mg MBAX)	0.064 ± 0.010	Traces
M_c [a] $\times 10^3$ (g/mol)	-	24 ± 0.4
ρ_c [b] $\times 10^{-6}$ (mol/cm^3)	-	59 ± 0.2
ξ [c] (nm)	-	52 ± 1.1

[a] Molecular weight between two cross-links; [b] Cross-linking density; [c] Mesh size; All values are means $\pm$ standard deviation of three repetitions.

The nitrogen adsorption/desorption isotherm of the MBAX microspheres is presented in Figure 4a. The N_2 adsorption measurements indicate that the specific surface area of MBAX microspheres is 11.19 m^2/g, beside; the isotherm was type IV, denoting the presence of mesopores [36]. Furthermore, a broad hysteresis loop associated with a desorption step above the relative pressure of 0.5 shown in N_2-isotherm is characteristic of a mesoporous organization. The calculation of pore size distribution in MBAX microspheres was based on the BJH method using the desorption isotherms (Figure 4b). The average pore size in microspheres was 30.8 nm, a value consistent with the mesoporous structure calculated from swelling experiments (Table 1). However, it should be emphasized that the absence of a plateau at high pressures in the isotherms and a non-Gaussian pore diameter distribution (Figure 4a,b) indicates a macroporous material. Nevertheless, it could also be attributed to apparent porosity, which could produce macro-cavities. These results confirm the heterogeneous microtexture observed in the SEM micrographs.

Figure 4. Textural analysis of MBAX microspheres. **(a)** Isotherm; **(b)** Pore size distribution.
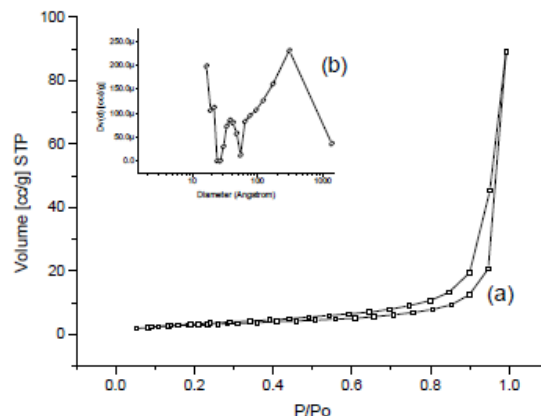
Experimental

Materials:

Maize bran arabinoxylans (MBAX) were obtained and characterized as previously reported [35]. MBAX contain 85% dry basis (d.b.) of pure AX. MBAX presented a ferulic acid (FA), di-FA, and tri-FA content of 0.25, 0.14, and 0.07 µg/mg of MBAX, respectively, and an A/X ratio of 0.72. Laccase (benzenediol: oxygen oxidoreductase, E.C.1.10.3.2) from Trametes versicolor and all other chemical products were purchased from Sigma Chemical Co. (St. Louis, MO, USA).

Methods:

MBAX Gelation: The reaction mixtures contained MBAX solution at 4% (w/v) in 0.1 M acetate buffer pH 5, laccase (1.670 nKat/mg of MBAX).

Rheological Tests: The formation of the MBAX gel was followed using a strain-controlled rheometer (Discovery HR-3 rheometer, TA Instruments, New Castle, DE, USA) in oscillatory mode as follows: cold (4 °C) solutions of 4% (w/v) MBAX were mixed

with laccase and immediately placed in the cone and plate geometry (5.0 cm in diameter, 0.04 rad in cone angle) maintained at 4 °C. MBAX gelation kinetic was started by a sudden increase in temperature from 4 to 25 °C and monitored at 25 °C for 6 h by following the storage (G') and loss (G'') modulus and tan δ (G''/G'). All measurements were carried out at a frequency of 0.25 Hz and 5% strain (linearity range of visco-elastic behavior). Frequency sweep (0.01–10 Hz) was carried out at the end of the network formation at 5% strain and 25 °C.

Covalent Cross-Links Content: FA, di-FA and tri-FA contents in MBAX microspheres were quantified by reverse phase highperformance liquid chromatography (RP-HPLC) after a deesterification step, as described elsewhere [12,18]. An Alltima (Alltech, Deerfield, IL, USA) C18 column (250 × 4.6 mm) and a photodiode array detector Waters 996 (Millipore Co., Milford, MA, USA) were used to record the ferulic acid and its di-FA and tri-FA spectra. Detection was by UV absorbance at 320 nm. Gradient elution was performed using acetonitrile and sodium acetate buffer 0.05 M, pH 4.0, at 1 mL/min at 35 °C, in linear gradients from 15:85 to 35:65 in 30 min, from 35:65 to 60:40 in 0.5 min, from 60:40 to 15:85 in 4.5 min, and finally maintained at 15:85 for 5 min.

MBAX Microspheres:

MBAX microspheres were prepared as previously described [23]. Briefly, the MBAX solution 4% (w/v) in 0.1 M acetate buffer pH 5 was mixed with 1.670 nKat/mg of MBAX. This reaction mixture was transferred to a syringe and equilibrated for approximately 4 min. Microspheres were obtained by dropwise extrusion into a hydrophobic liquid. The microspheres were aged for 12 h in this liquid at 25 °C under

stirring. Afterwards MBAX microspheres were collected and washed with water–ethanol (1:1) in order to remove the residual hydrophobic liquid from the microsphere surface and then freeze-dried.

Phase-Contrast Optical Microscopy: The MBAX microspheres shape and size were estimated using an optical microscope (Olympus-BX51, Olympus American Inc., Center Valley, PA, USA). The particle size of MBAX microspheres was determined by a stage micrometer having an accuracy of 0.01 mm. The average sizes of 100 MBAX microspheres were registered. Pictures in dark-field were taken and the microspheres size distribution was analyzed according to a reference scale.

Swelling and structural Parameters: After gelation, the MBAX microspheres were recovered by filtration, placed in glass vials and weighted. The MBAX microspheres were allowed to swell as described elsewhere [17]. The equilibrium swelling was reached when the weight of the samples changed by no more than 3% (0.06 g). The swelling ratio (q) was calculated by Equation (1):

$$q = (W_s - WMBAX)/WMBAX \qquad (1)$$

where W_s is the weight of swollen gels and WMBAX is the weight of MBAX in the gel. From swelling measurements, the molecular weight between two cross-links (M_c), the cross-linking density (ρc) and the mesh size (ϑ) values of the different MBAX gels were obtained as reported elsewhere [17]. Mc, ρc, and ϑ were calculated using the model of Flory and Rehner (1943) [37] modified by Peppas and Merrill [38] for gels where the cross-links are introduced in solution

To determine the nature of water diffusion into the microsphere, the following equation was used [37]:

$$M_t/M_o = k\, t^n \qquad\qquad (2)$$

where Mt is the weight of MBAX microspheres at time t, Mo is the initial weight of MBAX microspheres, k is the kinetic constant, and n is the dissolution exponent that characterizing the system. A value $n < 0.45$ indicate a Fickian diffusion mechanism, while $0.45 < n < 1$ indicate that a non Fickian or anomalous mechanism [39].

Scanning Electron Microscopy (SEM):

The surface morphology and microstructure of the freeze-dried MBAX microspheres was studied by field emission scanning electron microscopy (JEOL JSM-7401F, Peabody, MA, USA) without coating at low voltage (1.8 kV). SEM images were obtained in secondary and backscattered electrons image mode.

Textural analysis:

The textural analysis was conducted by adsorption/desorption of nitrogen. Surface area was determined by using nitrogen adsorption at their condensation temperature (77.35 °K) and at a relative pressure (p/p0) of 0.5–0.22 by the BET method [40]. The complete isotherm was conducted at $p/p_0 = 0.5$–0.99 for adsorption and p/p0 = 0.995–0.05 for desorption. A surface characterization Autosorb-1 (Quantachrome Instruments, Boynton Beach, FL, USA) was used. The surface of the samples was cleaned at 100 °C for 2 h under vacuum.

Statiscal Analysis: All measurements were made in triplicate and the coefficients of variation were lower than 8%. Results are expressed as mean values.

Conclusions

This study demonstrated that spherical and non-aggregated MBAX microspheres with an average diameter of 531 μm and an average mesh size of 52 nm can be prepared by enzymatic cross-linking. The MBAX microspheres present a porous structure featuring a heterogeneous organization. These structural and textural features confer to MBAX microspheres a high potential for application as microencapsulation systems for bioactive compounds.

Acknowledgments

References

1. Dai, C.; Wang, B.; Zhao, H. Microencapsulation peptide and protein drugs delivery system. Colloids Surf. B Biointerfaces 2005, 41, 117–120.

2. Zhang, H.; Alsarra, I.A.; Neau, S.H. An in vitro evaluation of a chitosan-containing multiparticulate system for macromolecule delivery to the colon. Int. J. Pharm. 2002, 239, 197–205.

3. Yang, L.; Chu, J.S.; Fix, J. Colon-specific drug delivery: New approaches and in vitro/in vivo evaluation. Int. J. Pharm. 2002, 235, 1–15.

4. Liu, Z.; Jiao, Y.; Wang, Y.; Zhou, C.; Zhang, Z. Polysaccharides-based nanoparticles as drug delivery systems. Adv. Drug Delivery Rev. 2008, 60, 1650–1662.

5. Sinha, V.R.; Singla, A.K.; Wadhawan, S.; Kaushik, R.; Kumria, R.; Bansal, K.; Dhawan, S. Chitosan microspheres as a potential carrier for drugs. Int. J. Pharm. 2004, 274, 1–33.

6. Sinha, V.R.; Kumria, R. Polysaccharides in colon-specific drug delivery. Int. J. Pharm. 2001, 224, 19–38.

7. Silva, C.M.; Ribeiro, J.; Vit, I. Alginate microspheres prepared by internal gelation: Development and effect on insulin stability. Int. J. Pharm. 2006, 311, 1–10.

8. Sinha, V.R.; Trehan, A. Biodegradable microspheres for protein delivery. J. Control. Release 2003, 90, 261–280.

9. Peppas, N.A. Hydrogels and drug delivery. Curr. Opin. Colloid Interface Sci. 1997, 2, 531–537.

10. Izydorczyk, M.S.; Biliaderi, C.G. Cereal arabinoxylans: Advances in structure and physicochemical properties. Carbohydr. Polym. 1995, 28, 33–48.

11. Smith, M.M.; Hartley, R.D. Occurrence and nature of ferulic acid substitution of cell-wall

polysaccharides in graminaceous plants. Carbohydr. Res. 1983, 118, 65–80.

12. Vansteenkiste, E.; Babot, C.; Rouau, X.; Micard, V. Oxidative gelation of feruloylated

arabinoxylan as affected by protein. Influence on protein enzymatic hydrolysis. Food

Hydrocolloid.

2004, 18, 557–564.

13. Schooneveld-bergmans, M.E.F.; Dignum, M.J.W.; Grabber, J.H.; Beldman, G. Studies on the

oxidative cross-linking of feruloylated arabinoxylans from wheat flour and wheat bran.

Carbohydr. Polym. 2008, 38, 309–317.

14. Martínez-López, A.L.; Carvajal-Millan, E.; Lizardi-Mendoza, J.; López-Franco, Y.L.;

Rascón-Chu, A.; Salas-Muñoz, E.; Barron, C.; Micard, V. The peroxidase/H2O2 system as a free

radical-generating agent for gelling maize bran arabinoxylans: Rheological and structural

properties. Molecules 2011, 16, 8410–8418.

15. Carvajal-Millan, E.; Rascón-Chu, A.; Márquez-Escalante, J.A.; Micard, V.; León, N.P.D.;

Gardea, A. Maize bran gum: Extraction, characterization and functional properties. Carbohydr. Polym.

2007, 69, 280–285.

16. Carvajal-Millan, E.; Guilbert, S.; Morel, M.-H.; Micard, V. Impact of the structure of arabinoxylan

gels on their rheological and protein transport properties. Carbohydr. Polym. 2005, 60,

431–438.

17. Carvajal-Millan, E.; Landillon, V.; Morel, M.-H.; Rouau, X.; Doublier, J.-L.; Micard, V.

Arabinoxylan gels: Impact of the feruloylation degree on their structure and properties.

Biomacromolecules 2005, 6, 309–317.

18. Bunzel, M.; Ralph, J.; Funk, C.; Steinhart, H. Structural elucidation of new ferulic acid-containing

phenolic dimers and trimers isolated from maize bran. Tetrahedron Lett. 2005, 46, 5845–

5850.

19. Carvajal-Millan, E.; Guilbert, S.; Doublier, J.-L.; Micard, V. Arabinoxylan/protein gels: Structural,

rheological and controlled release properties. Food Hydrocolloid. 2006, 20, 53–61.

20. Berlanga-Reyes, C.M.; Carvajal-Millán, E.; Lizardi-Mendoza, J.; Rascón-Chu, A.;

Marquez-Escalante, J.A.; Martínez-López, A.L. Maize arabinoxylan gels as protein delivery

matrices. Molecules 2009, 14, 1475–1482.

21. Iravani, S.; Fitchett, C.S.; Georget, D.M.R. Physical characterization of arabinoxylan powder and

its hydrogel containing a methyl xanthine. Carbohydr. Polym. 2011, 85, 201–207.

22. Hernández-Espinoza, A.B.; Piñón-Muñiz, M.I.; Rascón-Chu, A.; Santana-Rodríguez, V.M.; Carvajal-Millan, E. Lycopene/arabinoxylan gels: Rheological and controlled release characteristics. Molecules 2012, 17, 2428–2436.

23. Martínez-López, A.L.; Carvajal-Millan, E.; Lizardi-Mendoza, J.; López-Franco, Y.L.;

Rascón-Chu, A.; Micard, V. Laccase Induced Cross-Linking Arabinoxylans Microspheres. In Proceedings of the 11th International Food Hydrocolloids Conference: Biofunctionality and Technofunctionality of Hydrocolloids, Purdue, IN, USA, 15–18 May 2012.

24. Berlanga-Reyes, C.M.; Carvajal-Millán, E.; Caire Juvera, G.; Rascón-Chu, A.;

Marquez-Escalante, J.A.; Martinez-Lopez, A.L. Laccase induced maize bran arabinoxylans gels:

Structural and rheological properties. Food Sci. Biotechnol. 2009, 18, 1027–1029.

25. Niño-Medina, G.; Carvajal-Millán, E.; Lizardi, J.; Rascon-Chu, A.; Marquez-Escalante, J.A.; Gardea, A.; Martinez-Lopez, A.L.; Guerrero, V. Maize processing waste water arabinoxylans: Gelling capability and cross-linking content. Food Chem. 2009, 115, 1286–1290.

26. Lapierre, C.; Pollet, B.; Ralet, M.C.; Saulnier, L. The phenolic fraction of maize bran: Evidence for lignin-heteroxylan association. Phytochemistry 2001, 57, 765–772.

27. Fundueanu, G.; Esposito, E.; Mihai, D.; Carpov, A.; Desbrieres, J.; Rinaudo, M.; Nastruzzi, C.

Preparation and characterization of Ca-alginate microspheres by a new emulsification method.

Int. J. Pharm. 1998, 170, 11–21.

28. Grishechko, L.I.; Amaral-Labat, G.; Szczurek, A.; Fierro, V.; Kuznetsov, B.N.; Pizzi, A.; Celzard, A.

New tannin-lignin aerogels. Ind. Crops Prod. 2013, 41, 347–355.

29. Chen, F.; Li, J. Synthesis and structural characteristics of organic aerogels with different content

of lignin. Adv. Mater. Res. 2010, 113–116, 1837–1840.

30. Chen, F.; Xu, M.; Wang, L.; Li, J. Preparation and characterization of organic aerogels from a lignin–resorcinol–formaldehyde copolymer. Bioresources 2011, 6, 1261–1272.

31. Al-Muhtaseb, S.A.; Ritter, J.A. Preparation and properties of resorcinol-Formaldehyde organic and carbon gels. Adv. Mater. 2003, 15, 101–114.

32. Raschip, I.E.; Hitruc, E.G.; Oprea, A.M.; Popescu, M.C.; Vasile, C. In vitro evaluation of the mixed xanthan/lignin hydrogels as vanillin carriers. J. Mol. Struct. 2011, 1003, 67–74.

33. Barakat, A.; Putaux, J.-L.; Saulnier, L.; Chabbert, B.; Cathala, B. Characterization of arabinoxylans-dehydrogenation (synthetic lignin polymer) polymer nanoparticles. Biomacromolecules

2007, 8, 1236–1245.

34. Berlanga-Reyes, C.M.; Carvajal-Millan, E.; Lizardi-Mendoza, J.; Islas-Rubio, A.R.; Rascón-Chu, A.

Enzymatic cross-linking of alkali extracted arabinoxylans: Gel rheological and structural

characteristics. Int. J. Mol. Sci. 2011, 12, 5853–5861.

35. Martinez-Lopez, A.L.; Carvajal-Millan, E.; Lizardi-Mendoza, J.; Rascón-Chu, A.;

López-Franco, Y.L.; Salas-Muñoz, E. Ferulated Arabinoxylans as By-Product from Maize

Wet-Milling Process: Chacterization and Gelling Capability. In Maize: Cultivation, Uses and Health

Benefits; Jimenez-Lopez, J.C., Ed.; Nova Science Publisher: Granade, Spain, 2012; pp. 65–74.

36. Gregg, S.J.; Sing, K.S.W. Adsortion, Surface Area and Porosimetry, 2nd ed.; Academic Press Inc.:

London, UK, 1991.

37. Flory, P.J.; Rehner, J. Statistical mechanics of cross-linked polymer networks I. rubberlike elasticity. J. Chem. Phys. 1943, 11, 512.

38. Peppas, N.A.; Merrill, E.W. Poly(vinyl alcohol) hydrogels: Reinforcement of radiation-crosslinked networks by crystallization. J. Polym. Sci. Polym. Chem. 1976, 14, 441–457.

39. Peppas, N.A. Analysis of Fickian and non-Fickian drug release from polymers. Phram. Acta Helv.

1985, 60, 110–111.

40. Brunauer, S.; Emmett, P.H.; Teller, E. Asorption of gases in multimolecular layers. J.

Am. Chem. Soc.

1938, 60, 309–319.